ON THE MECHANICAL VIBRATIONS OF A RIBBON LOUDSPEAKER'S STRIP WHIT RECTANGULAR SHAPE: CASE STUDY

[a)]Iliyan Iliev

[a)]Nikola Vaptsarov Naval Academy, Varna, Bulgaria, i.y.iliev@naval-acad.bg

Abstract: This paper presents a case study focusing on the vibrations of a ribbon loudspeaker's strip. These vibrations induce surface deformation, resulting in a degradation of the reproduced sound quality. The phenomenon is briefly reviewed, and the theoretical foundations are outlined. Several modes of the loudspeaker's strip are analyzed using 3D and 2D simulations conducted in Matlab® and COMSOL Multiphysics. A video recording has been done that visually demonstrates the specific modes that were theoretically calculated. Conclusions drawn from the mode analysis are applicable to the design and manufacturing of loudspeakers.

Keywords: Eigenfrequencies, Modes, Ribbon Loudspeaker, Rectangular Plate, Vibrations.

1. INTRODUCTION

Unlike loudspeakers with a circular piston [1-4], those with a rectangular strip are more prone to breaking when its surface is deformed under the influence of its eigenfrequencies.

This paper focuses on the mechanical vibrations of a rectangular strip of the loudspeaker. These vibrations result in deformations, or modes, on the strip's surface, impacting the quality of reproduced sound and potentially posing a risk of its destruction.

Understanding the critical points (certain modes) that may compromise the structural integrity of loudspeakers with rectangular strip is essential. This knowledge enables the implementation of quality control measures (active filters) or other protective strategies to maintain the performance and durability of these loudspeakers.

A brief review and the comprehensive theoretical basis for this phenomenon have been presented at the beginning of the paper. Further, several modes of the strip of a specific loudspeaker have been simulated, analyzed and visualized in 2D and 3D using Matlab® and COMSOL Multiphysics software programs. To do so, the Finite Elements Method (FEM) has been used, similar to [5].

Finally, an experiment has been conducted – video recording (at 60 fps) of some of the strip's modes.

2. THEORETICAL BACKGROUND

2. 1. The Basic Plate Theory

The acoustic mass and impedance of the ribbon loudspeaker depend on the reproduced frequency [6]. This results in resonances at different frequencies for a given ribbon loudspeaker. Those resonant frequencies are in relation to the strip's thickness.

Theoretically, the behavior of the ribbon loudspeaker's strip may be compared to that of a very thin (a few microns) plate. A plate is a solid body bounded by two parallel flat surfaces, having two dimensions far greater than the third [7, 8]. When the ratio of the plate thickness to its smaller lateral dimension (in this case, the width) is less than 1/20, the plate is usually considered to be thin [9].

There are two main mathematical methods for plate modes examination. The first method, as proposed by Poisson, involves the development of a series of functions representing stress and strain along the Z coordinate (Fig. 1), a concept originally established by Cauchy. The second is based on Kirchhoff's General Theory of thin rods or wires represented by Love, generalized for different plate thickness by Midlin (and now known as Midlin Plate Theory).

These two approaches consider deformations of the plates whose edges are either clamped or simply supported, while more sophisticated methods like the Rayleigh-Ritz method, Finite Strip method, Two-new eigenfunction theory, to name a few, examine plates with all possible combinations of clamped, simply supported, and free edge conditions [10, 11].

There are also other approaches for analyzing thin plate vibrations, like the Bessel function method, where various Bessel functions represent the different mechanical vibrations (modes) with different boundary conditions [12]. The first of the strip's modes has the highest amplitude, while the actual deformations of the other modes are significantly smaller [9].

Therefore, the deformation of the strip in the first eigenfrequency (first mode) will be of most significant research interest in terms of both – the mechanical bending of the strip and the degree of deterioration of the reproduced sound.

In the current paper, the Rayleigh Method has been used to determine the first eigenfrequency of the ribbon loudspeaker. The obtained result has been compared to results from simulations conducted by software products using the Basic Plates Theory for calculating the resonant frequencies. It also has been compared to the 60-fps video recording of the plate mechanical vibrations.

In Basic Plates Theory, some intensities and moments pertain to a unit length of the cross-section [13, 14]. Those are:

– shear forces – Q_x and Q_y;

– bending moments – M_x and Q_y;

– twisting moments – $M_{xy} = M_{yx}$.

In Fig. 1, the latter are shown, including tangential stresses (σ_x, σ_{xy}, σ_{xz}, σ_y, σ_{yx} and σ_{yz}) on the surface of the plate.

The numerical values of the intensities and moments on the plate surface are [13, 14]:

$$\begin{aligned} \boldsymbol{Q_x} &= \int_{-\frac{h}{2}}^{\frac{h}{2}} \boldsymbol{\sigma_{xz} dz}\,, \boldsymbol{Q_y} = \int_{-\frac{h}{2}}^{\frac{h}{2}} \boldsymbol{\sigma_{yz} dz}; \\ \boldsymbol{M_x} &= \int_{-\frac{h}{2}}^{\frac{h}{2}} \boldsymbol{z\sigma_y dz}\,, \boldsymbol{M_y} = \int_{-\frac{h}{2}}^{\frac{h}{2}} \boldsymbol{z\sigma_x dz}; \\ \boldsymbol{M_{xy}} &= \boldsymbol{M_{yx}} = \int_{-\frac{h}{2}}^{\frac{h}{2}} \boldsymbol{z\sigma_{xy} dz}, \end{aligned} \tag{1}$$

where h is the plate thickness.

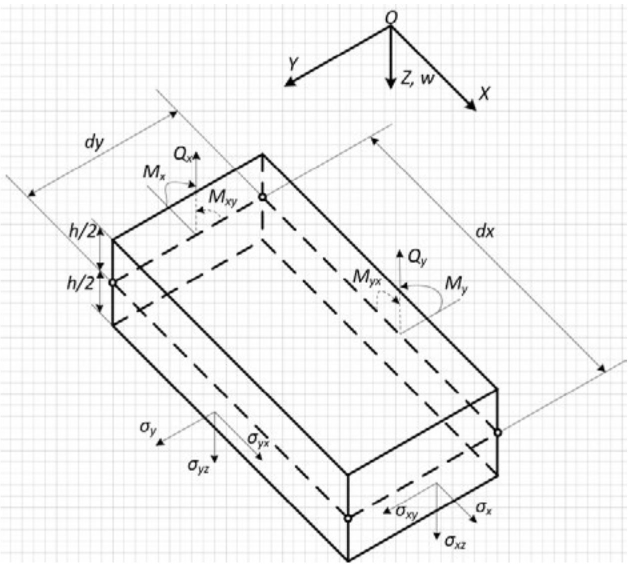

Fig. 1: Shear forces, bending and twisting moments and tangential stresses

Due to the plane-strained state of the plate, the tangential stresses σ_z, σ_{zx} and σ_{zy}, will be considerably smaller than σ_x, σ_y, and σ_{xy}, therefore they are neglected. The tangential stresses are known from Hook's law for the two-dimensional strained state [14]:

$$\begin{aligned} \boldsymbol{\sigma_x} &= \frac{\boldsymbol{E}}{\boldsymbol{1-v^2}}(\boldsymbol{\varepsilon_x + v\varepsilon_y}); \\ \boldsymbol{\sigma_y} &= \frac{\boldsymbol{E}}{\boldsymbol{1-v^2}}(\boldsymbol{\varepsilon_y + v\varepsilon_x}); \\ \boldsymbol{\sigma_{xy}} &= \frac{\boldsymbol{E}}{\boldsymbol{2(1+v)}}\boldsymbol{\varepsilon_{xy}} \end{aligned} \tag{2}$$

where υ is Poisson's ratio, characterizing the elastic properties of the material;

E – Young's modulus.

In Eq. (2) ε_x, ε_y and ε_{xy} are the correlations between the movements and the deformations. Those strain-displacement relations that result in the elastic body being strained due to the applied load are well known from Cauchy's work:

$$\begin{aligned}\varepsilon_x &= \frac{du}{dx};\\ \varepsilon_y &= \frac{dv}{dy};\\ \varepsilon_{xy} &= \frac{du}{dy}+\frac{dv}{dx},\end{aligned} \tag{3}$$

where u and v represent the horizontal movements, subsequently on the X and Y axis, of that point on the plate's surface.

After applying Eq. (3) in Eq. (2) and then Eq. (2) in Eq. (1) and afterward integrating to the plate's thickness (on Z) one obtains:

$$\begin{aligned}M_x &= -D\left(\frac{d^2w}{dx^2}+\upsilon\frac{d^2w}{dy^2}\right);\\ M_y &= -D\left(\frac{d^2w}{dy^2}+\upsilon\frac{d^2w}{dx^2}\right);\\ M_{xy} &= -D(1-\upsilon)\frac{d^2w}{dxdy}\end{aligned} \tag{4}$$

where $w(x,y)$ is a displacement function;

$D = \dfrac{Eh^3}{12(1-\upsilon^2)}$ – plate stiffness (flexural rigidity of the plate material).

The internal forces and moments can be related when considering equilibrium of the plate elements. Thus, for equilibrium in the X direction, in the absence of body forces [7]:

$$\frac{d\sigma_x}{dx}+\frac{d\sigma_{xy}}{dy}+\frac{d\sigma_{xz}}{dz}=0. \tag{5}$$

After multiplying Eq. (5) by z and integrating over the thickness of the plate one can assume that:

$$Q_x = \frac{dM_x}{dx}+\frac{dM_{xy}}{dy} \tag{6}$$

Similarly, one can integrate the equation of equilibrium in the Y direction:

$$Q_y = \frac{dM_y}{dy}+\frac{dM_{xy}}{dx} \tag{7}$$

Considering the integration over the thickness of the last equilibrium equations in the Z direction one obtains:

$$\frac{d\sigma_{xz}}{dx}+\frac{d\sigma_{yz}}{dy}+\frac{d\sigma_{zz}}{dz}=0, \tag{8}$$

Integrating the equation of equilibrium in the Z direction, one obtains:

$$\frac{dQ_x}{dx}+\frac{dQ_y}{dy}+q(x,y)=0 \tag{9}$$

where $q(x,y)$ is a normal load distribution on the top face of the plate.

After replacing Equations (4), (7) and (8) in Eq. (9) one obtains the nonhomogeneous biharmonic equation of Sophie-Germaine for a plate with constant thickness:

$$\frac{d^4w}{dx^4}+2\frac{d^4w}{dx^2dy^2}+\frac{d^4w}{dy^4}+\frac{q}{D}=0 \tag{10}$$

Equation (10) is also known as equation of motion or Euler-Lagrange equation and is usually written as:

$$\nabla^4 w = \frac{q}{D} \tag{11}$$

where ∇^4 is the biharmonic operator (∇^2 – Laplacian operator).

When the displacement function w(x,y) is known, the deformation form (mode shape) can be represented. This function can be calculated after integrating the equation of motion Eq. (10) for specific boundary conditions. The roots of the equation will then be resonant (natural) frequencies.

The current article deals with a ribbon loudspeaker whose plate edges are fixed–free–fixed–free, as illustrated in Fig. 2.

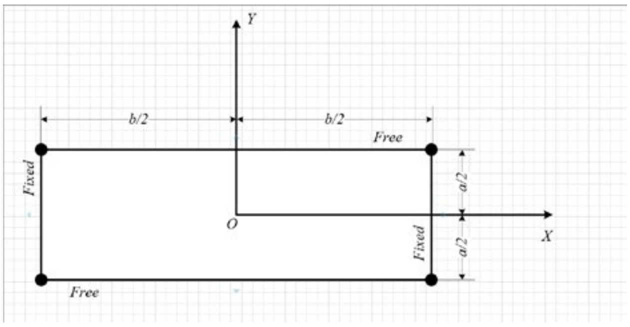

Fig. 2: The boundary conditions of the plate edges

The boundary conditions for calculating the displacement function after integrating the equation of motion for the case at hand (Fig. 2) are [7]:

$$\begin{aligned} &w(-b/2, y) = 0; \\ &w(+b/2, y) = 0; \\ &\frac{dw}{dx} = 0, \text{for } (\pm b/2, y). \end{aligned} \tag{12}$$

Then, the bending moment M_y and the shear force Q_y on the Y axis are:

$$\begin{aligned} &M_y = -D\left(\frac{d^2w}{dy^2} + v\frac{d^2w}{dx^2}\right) = 0;\ for\ (x, \pm a/2) \\ &Q_y = D\frac{d}{dy}[\nabla^2 w] = -D\frac{d}{dy}\left\{\left[\frac{d^2}{dx^2} + \frac{d^2}{dy^2}\right]w\right\} = 0. \end{aligned} \tag{13}$$

Considering the given boundary conditions, and if one replaces $w(x,y,t)=W(x,y)e^{j\omega t}$ in Eq. (10), the biharmonic equation of a plate with constant thickness will be [14]:

$$\frac{d^4W}{dx^4} + 2\frac{d^4W}{dx^2dy^2} + \frac{d^4W}{dy^4} + \rho h\frac{\omega^2 W}{D} = 0, \tag{14}$$

where ω is angular frequency;

ρ – density of the material.

Due to a certain degree of difficulty when solving differential equations of that order, approximate methods for calculating the resonant frequencies and representing the mode shape are used.

2. 2. The Rayleigh Method for plates

In the Rayleigh Method, the displacement function is represented by two equations – for strain energy and kinetic energy. With this method, only the upper limit of the fundamental frequency for the first mode can be calculated.

The total kinetic energy of a freely vibrating plate with natural frequency ω=ω_1 is [7]:

$$T = \frac{1}{2}\int_{-\frac{b}{2}}^{\frac{b}{2}}\int_{-\frac{a}{2}}^{\frac{a}{2}} \rho h\dot{w}(x, y, t)dxdy. \tag{15}$$

A solution of the form is assumed as $w(x,y,t)=W(x,y)e^{j\omega t}$ and thus Eq. (15) can be rewritten:

$$T = \frac{\omega^2}{2}\int_{-\frac{b}{2}}^{\frac{b}{2}}\int_{-\frac{a}{2}}^{\frac{a}{2}} \rho h W_1^2(x, y)dxdy. \tag{16}$$

Eq. (16) will have maximum value when $\sin^2\omega_1 t=1$.

The maximum total strain energy V_{max} of the plate is [7]:

$$\begin{aligned} &V\frac{D}{2}\int_{-\frac{b}{2}}^{\frac{b}{2}}\int_{-\frac{a}{2}}^{\frac{a}{2}}(\nabla^2 W_1)^2 dxdy \\ &\qquad\qquad max \\ &\frac{D}{2}\int_{-b/2}^{b/2}\int_{-a/2}^{a/2}\left[2(1-v)\left\{\left(\frac{d^2W_1}{dxdy}\right)^2 - \frac{d^4W_1}{dx^2dy^2}\right\}\right]dxdy. \end{aligned} \tag{17}$$

For a conservative system by Rayleigh's principle [15] one can equalize the maximum kinetic energy Eq. (16) and maximum strain energy Eq. (17) of the system and extract the natural frequency ω=ω_1, so:

$$\omega_1^2 = \frac{D\int_{-b/2}^{b/2}\int_{-a/2}^{a/2}[(\nabla^2 W_1)^2 + 2(1-v)\{W_{1,xy}^2 - W_{1,xx}W_{1,yy}\}]dxdy}{\rho h\int_{-b/2}^{b/2}\int_{-a/2}^{a/2} W_1^2 dxdy}, \tag{18}$$

where: , are Rayleigh's Quotient and give the fundamental natural frequency of the plate.

The Rayleigh method's accuracy can be improved using the Rayleigh–Ritz method or other more sophisticated methods to calculate all resonant frequencies.

3. EXPERIMENTAL SETUP AND RESULTS

Matlab® and COMSOL Multiphysics were used to calculate the resonant frequencies and to simulate the corresponding mode shapes on the surface of the plate. Both software products use Basic Plate Theory for the calculations.

Frequency generator, Power Amplifier, Ribbon Loudspeaker-VLD 40, DAQ System, Digital Multimeter and a High-speed Camera (60 fps) are used for video recording of the modes (the experimental setup is shown in Fig. 3).

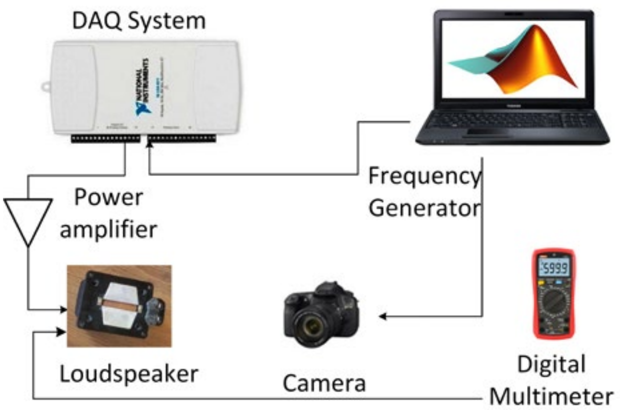

Fig. 3: Experimental setup diagram

The properties of the loudspeaker's plate are given in Tab. 1.

Young's Modulus, GPa	70
Poisson's Ratio	0.33
Mass Density, kg/m^3	2700
Thickness, mm	0.014
Width, mm	8.6
Length, mm	56
Material	Aluminum

Tab. 1: Plate Properties

For better understanding and accuracy of the comparative analysis the author demonstrates one more method for calculating the first natural frequency - the Rayleigh Method. (A Matlab® based software program is used [16]). The calculations point that the natural frequency of a plate in the case study is 24 Hz.

In Tab. 2 resonant frequencies and corresponding distortion, the resonant frequencies and their corresponding mode shapes are represented. Those are calculated using Matlab® and COMSOL Multiphysics products which uses FEM to implement the Basic Plate Theory.

The video recording, where some of the calculated modes are visible, is available in [17]. A careful review of the video recording reveals detectable distortions in the plate.

The most pronounced deformation is observed in the first mode at 24 Hz. Additionally, higher order modes such as the 7th mode at 312 Hz are also discernible.

Theoretical analysis, as depicted in Tab. 2, reveals that as the frequency rises, the deformations of the surface of the plate become more complex.

The complex combination of shear forces, bending and twisting moments and the fixed position of the short edges of the plate lead to various deformations on its surface.

4. CONCLUSION

The results represented in Tab. 2 and the calculated fundamental frequency by the Rayleigh Method [16] confirm the basic theory. The eigenfrequency (the frequency of the first mode) obtained through the Rayleigh Method is higher than the fundamental frequency obtained through Basic Plate Theory. Therefor, may affect the integrity of the plate (loudspeaker's strip).

The Matlab® program [16] utilizing the Rayleigh method provides only the first mode, characterized by the highest amplitude, but its accuracy is not particularly emphasized. Conversely, Basic Plate Theory offers higher accuracy and computes different eigenfrequencies.

The negligible disparities in frequency calculations between Matlab® and COMSOL Multiphysics result from the different quantities of finite elements employed (6656 for COMSOL Multiphysics and 576 for Matlab®).

As observed in video record [17], there exists a considerable plate displacement (first mode) at a 24 Hz frequency. This finding supports the outcome derived from numerical analysis of the first mode using both the Rayleigh Method and Basic Plate Theory. Yet, due to limitations in the recording equipment, most of the higher modes remain indistinct.

The simulations, mode shape analysis, and experimental observations captured in the video recording enhance theoretical understanding. The findings of this research hold relevance in the realm of designing and manufacturing ribbon loudspeakers.

№	Freq., Hz	Matlab (3D)	Matlab (2D)	COMSOL (3D)	COMSOL (2D)
1	Matlab – 23.38 COMSOL – 23.87	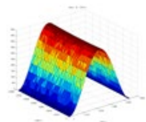	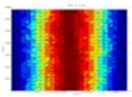	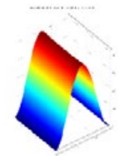	
2	Matlab – 64.51 COMSOL – 65.77	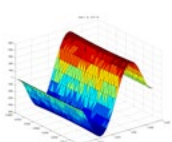	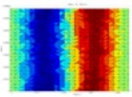	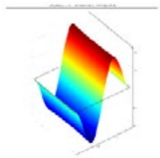	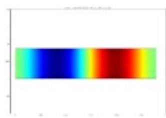
3	Matlab – 96.86 COMSOL – 98.90	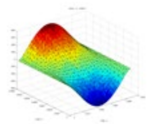	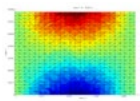	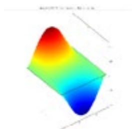	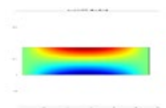
4	Matlab – 126.60 COMSOL – 129.17	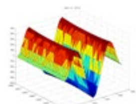	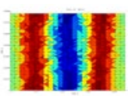	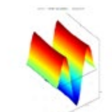	
5	Matlab – 197.70 COMSOL – 201.93	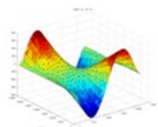	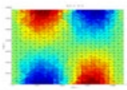	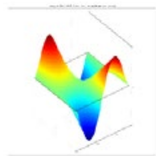	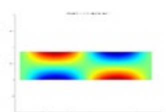
6	Matlab – 210.10 COMSOL – 214.13	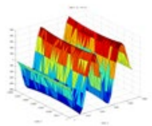	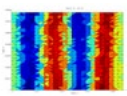	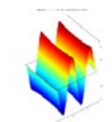	
7	Matlab – 306.00 COMSOL – 312.86	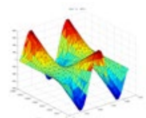	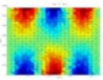	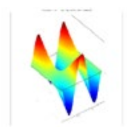	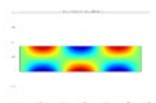
8	Matlab – 314.80 COMSOL – 320.88	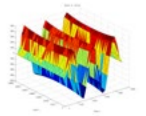	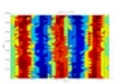	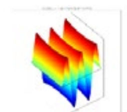	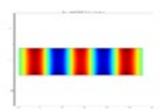

Tab. 2: Calculated resonant frequencies and corresponding distortion

ACKNOWLEDGEMENT

This research paper has received funding from Ministry of Education and Science of the Republic of Bulgaria under the National Science Program "SECURITY AND DEFENSE", in implementation of the Decision of the Council of Ministers of the Republic of Bulgaria No: 731/21.10.2021 and according to Agreement No: D01-74/19.05.2022.

REFERENCES

G. Liyang, T. Li, H. Meiying, H. Yilong. (2024). Distributed Two modes of motions for a single disk on the vibration stage. *J. Phys.: Condens. Matter 36*, 2024: 10.

https://doi.org/10.1088/1361-648X/ad1135

G. Liyang, T. Li, H. Meiying, H. Yilong. Dynamics of a vibration-driven single disk. *Scientific Reports 11(1),*2021: 16561.

https://doi.org/10.1038/s41598-021-95672-6

W. Klippel. Distributed Mechanical Parameters Describing Vibration and Sound Radiation of Loudspeaker Drive Units. *International Symposium on ElectroAcoustic Technologies,* Shenzhen, China, 2009.

W. Duan, C. Wang, C. Wang. Modification of fundamental vibration modes of circular plates with free edges. *Journal of Sound and Vibration,* 2008: 709-715.

https://doi.org/10.1016/j.jsv.2008.03.065

B. Vanam, M. Rajyalakshmi, R. Inala. (2012). Static analysis of an isotropic rectangular plate using finite element analysis (FEA). *Journal of Mechanical Engineering Research*, 4 (4), 2012: 148– 162.

https://doi.org/10.5897/JMER11.088

L. Beranek, J. Mellow. Acoustics: Sound Fields and Transducer. *Academic Press,* 2019.

S. Chakraverty. Vibration of Plates. *Taylor&Francis Group,* Boca Raton, 2009.

S. Chakraverty. Vibration of Functionally Graded Beams and Plates. *Academic Press,* 2016.

S. Prasad, B. Ranghavendra. Determination of Fundamental Frequency of a Thin Rectangular Plate by Using COMSOL Multiphysics. *COMSOL Conference,* Bangalore, 2011.

Y. Xing, B. Liu. Closed form solutions for free vibrations of rectangular Midlin plates. *The Chinese Society of Theoretical and Applied Mechanics and Springer-Verlag,* 2009: 689– 698.

https://doi.org/10.1007/s10409-009-0253-7

S. Hashemi S., M. Arsanjani. Exact characteristic equations for some of classical boundary conditions of vibrating moderately thick rectangular plates. *International Journal of Solids and Structures*, Vol. 42, 2005: 819– 853.

https://doi.org/10.1016/j.ijsolstr.2004.06.063

J. Wu, A. Liu, H. Chen. Exact Solutions for Free-Vibration Analysis of Rectangular Plates Using Bessel Functions. *Journal of Applied Mechanics,* 74, 2007: 1247– 1251.

https://doi.org/10.1115/1.2744043

J. Maksimov, D. Duncheva, A. Antchev. Computer methods of engineering analysis. Part 2 – Linear Statics of not-beam structures. *And st Express,* Gabrovo, 2005 *(In Bulgarian).*

W. Soedel W. Vibrations of Shells and Plates. *3th ed. Taylor & Francis,* New York, 2005.

M. Geradin, D. Rixen. Mechanical Vibrations: Theory and Application to Structural Dynamics. *3th ed. John Wiley & Sons Ltd*, Chichester, 2015.

A Matlab GUI script for calculating the bending fundamental frequency of a rectangular plate. https://vibrationdata.wordpress.com/2012/12/14/plate– bending– frequency/ (Accessed 13.08.2024).

I. Iliev, "Vibrations of Thin Rectangular Plates", Mendeley Data, V1, 2024, https://doi.org/10.17632/3ysdzstccx.1 (Accessed 13.08.2024).

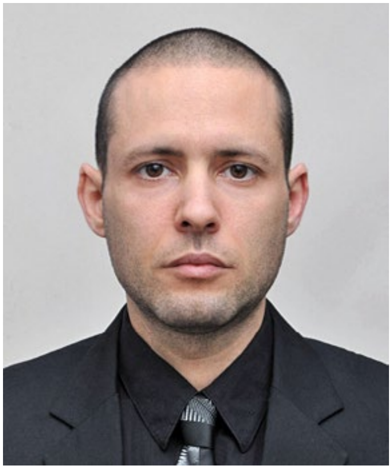

Iliyan Yordanov Iliev, PhD is a naval officer and faculty member at the Department of Information Technologies, Nikola Vaptsarov Naval Academy, Varna, Bulgaria. He holds a PhD in Communication Engineering and Technologies. His professional background includes service as a naval communications officer with expertise in radio systems, radiolocation and cryptography. He teaches computer science, cryptography, computer networks, and related disciplines. His research interests include cybersecurity, computer architectures, and the application of 3D printing, scanning and IoT technologies in maritime domain.